



Original Article

Novel water-assisting low firing MoO₃ microwave dielectric ceramicsDi Zhou^{a,b,*}, Li-Xia Pang^{a,c}, Da-Wei Wang^a, Ian M. Reaney^{a,*}^a Department of Materials Science and Engineering, University of Sheffield, S1 3JD, UK^b Electronic Materials Research Laboratory, Key Laboratory of the Ministry of Education & International Center for Dielectric Research, School of Electronic and Information Engineering, Xi'an Jiaotong University, Xi'an, 710049, China^c Micro-Optoelectronic Systems Laboratories, Xi'an Technological University, Xi'an, 710032, Shaanxi, China

ARTICLE INFO

Keywords:
Ceramics
Microwave dielectrics

ABSTRACT

MoO₃ ceramics can not be well densified via conventional solid state method and a low relative density (ρ) was obtained (~64.5% at 680 °C) with a permittivity (ϵ_r) ~ 7.58, a quality factor (Qf) ~ 35,000 GHz and a temperature coefficient of resonant frequency (TCF) ~ - 39 ppm/°C. However, cold sintering at 150 °C using 4 wt. % H₂O at 150 MPa enhanced densification and give a relative ρ ~ 76.8% and ϵ_r ~ 8.31 but with a Qf of only ~ 900 GHz. The addition of (NH₄)₆Mo₇O₂₄·4H₂O further improved densification to give a relative ρ ~ 83.7% after annealing at 700 °C, resulting in a ϵ_r ~ 9.91 with a Qf ~ 11,800 GHz. We conclude therefore that oxides that are difficult to be sintered via a conventional solid state route may benefit from cold sintering but despite the higher density, lower Qf cannot be avoided due to the impurities and grain boundary phases that are introduced.

1. Introduction

Low temperature co-fired ceramic (LTCC) technology has become an important fabrication method for modern electronic devices due the low cost of manufacture and potential of the integration multiple microwave (MW) circuits. [1–4] LTCCs are required to have lower sintering temperatures than that of the inner metal electrodes (typically Ag, 961 °C) [5,6] but classic MW dielectric ceramics typically densify at > 1000 °C. [1–7]. Lowering the sintering temperature of a MW ceramic by the addition of low-melting-point glasses and oxides has been used to fabricate many commercial LTCCs [1–7]. The search for intrinsically low sintering temperature LTCC has accelerated in recent years and the so-called family of ultra-LTCC (ULTCC) compounds can be well sintered at as low as 400 °C [8–11]. Most MW dielectric ceramics are oxides and their sintering temperatures are, to a simple approximation, determined by their melting points. Consequently, systems rich in low melting temperature oxides, such as TeO₂ (733 °C), MoO₃ (795 °C), Bi₂O₃ (817 °C), B₂O₃ (450 °C), P₂O₅ (340 °C) and V₂O₅ (690 °C), have been explored in the past decade [7–14].

Despite more than 50 types ULTCC molybdates have been reported to date, [8,10,12,14] the understanding of some simple binary compositions, such as MoO₃, is quite limited. MoO₃ powders are usually produced by roasting molybdenum disulfide in industry and take on a yellow color with a monoclinic crystal structure (space group *Pbnm*, $a = 3.962$ Å, $b = 13.855$ Å and $c = 3.696$ Å). [15,16] Its theoretical

density ρ is 4.692 g/cm³ [3] with a melting point 795 °C and many MoO₃-rich compounds have commensurately low melting points and sintering temperatures. However, when not alloyed with other binary compounds, MoO₃ can be well densified [10,14]. Even MoO₃-rich phases in well known phase diagrams, such as the Bi₂O₃-MoO₃ binary system, struggle to achieve high density, [10] e.g. Bi₂Mo₃O₁₂ which, despite its excellent MW properties (ϵ_r ~ 19, Qf ~ 21,800 GHz and TCF ~ - 215 ppm/°C), has never been synthesized with relative $\rho > 90\%$. However, Varghese et al. [13] have reported that MoO₃ sintered at 650 °C has a ϵ_r ~ 6.6 and a Qf ~ 41,000 GHz at 11.3 GHz and claimed a high relative ρ (~ 88%) was achieved via traditional sintering.

Most ceramics are processed using a conventional solid-state method using dry powders at high temperature. However, the poor sinterability of MoO₃ and its partial solubility in water suggest that a solution assisted method, i.e. cold sintering, [17,18] may be beneficial in achieving high ρ . Cold sintering can be explained as a room temperature crystallization or condensation from supersaturated solutions at grain boundaries, which has been employed in salt manufacture for more than one thousand years. The first successful microwave dielectric ceramic densified using cold sintering was Li₂MoO₄ [19,20]. The properties of Li₂MoO₄ conventionally sintered at 540 °C were first reported in our previous work [14] with a ϵ_r ~ 5.5, a Qf ~ 46,000 GHz and a TCF ~ - 160 ppm/°C. In 2014, Jantunen et al. [19] demonstrated that dense Li₂MoO₄ ceramic may be obtained at 80 °C if water is added. They also recognized that this approach permits the formation of

* Corresponding authors at: Department of Materials Science and Engineering, University of Sheffield, S1 3JD, UK.

E-mail addresses: zhoudi1220@gmail.com (D. Zhou), i.m.reaney@sheffield.ac.uk (I.M. Reaney).<https://doi.org/10.1016/j.jeurceramsoc.2019.01.052>

Received 8 October 2018; Received in revised form 29 January 2019; Accepted 30 January 2019

Available online 31 January 2019

0955-2219/© 2019 Elsevier Ltd. All rights reserved.

Li_2MoO_4 -rich composite ceramics, such as $\text{Li}_2\text{MoO}_4\text{-TiO}_2$, $\text{Li}_2\text{MoO}_4\text{-BaTiO}_3$ etc. [19–21] In 2016, Randall and his co-workers expanded this natural mechanism to other partially water-soluble MoO_3 and V_2O_5 based systems [17,18]. Solubility in water determines whether a material is suitable for cold sintering. Generally speaking, the cold sintering process (CSP) is a protocol for achieving dense ceramic solids by integrating particles, particle-fluid interface control and external pressure at very low temperatures. CSP uses a transient aqueous environment to achieve densification through a mediated dissolution-precipitation process. Although MoO_3 is only slightly water soluble, ammonium molybdate is highly soluble and decomposes to MoO_3 and NH_3 (g) above 370°C [22,23]. Hence, it may be an ideal accelerant for cold sintering of MoO_3 ceramics.

In the present work, a comparison is made between MoO_3 ceramics prepared via a conventional solid-state method and cold sintering using water / $(\text{NH}_4)_6\text{Mo}_7\text{O}_{24}\cdot 4\text{H}_2\text{O}$ additions. Their phase evolution, microstructure and MW dielectric properties are presented and discussed in detail.

2. Experimental section

2.1. Solid state reaction method

MoO_3 (> 99%, Fisher Scientific) were ball-milled for 24 h in isopropanol with ZrO_2 balls. After drying, the powders were pressed into cylinders (20 mm in diameter and 4 ~ 5 mm in height) at 30 ~ 50 MPa. Samples were sintered 2 h at 640–740 °C.

2.2. Cold sintering method

Fine MoO_3 powder was mixed with 4 wt. % water using an agate mortar. The mixture was pressed into cylinders (20 mm in diameter and 4 ~ 5 mm in height) at 100 ~ 150 MPa at $120 \sim 150^\circ\text{C}$ from 10 min to 30 min. Besides, 10 wt. % $(\text{NH}_4)_6\text{Mo}_7\text{O}_{24}\cdot 4\text{H}_2\text{O}$ was also mixed with MoO_3 powders and water (4 wt. %) and the same cold sintering process was carried out. To prevent the reaction between MoO_3 and the steel, thin PTFE pellets were added inside the die during the cold sintering process. After cold sintering, the samples were dried at 120°C for 24 h before measurements. Some samples were also annealed at 600 to 700°C in air after cold sintering.

2.3. Structural, microstructure and electrical characterization

Bulk density ρ was measured by the Archimedes' method (using ethanol as liquid) as well as by calculating the mass / volume from basic geometry. X-ray diffraction (XRD) was performed using with Cu K α radiation (Bruker D2 Phaser) from $5 - 65^\circ 2\theta$ at a step size of 0.02° . Natural and fractured surfaces were observed by scanning electron microscopy (SEM, FEI, Inspect F). Dielectric properties at MW frequency were measured using the $\text{TE}_{01\delta}$ dielectric resonator method with a network analyzer (Advantest R3767CH; Advantest, Tokyo, Japan) and a home-made heating system. The temperature coefficient of resonant frequency TCF (τ_f) was calculated with the following formula:

$$\text{TCF}(\tau_f) = \frac{f_T - f_{T_0}}{f_{T_0} \times (T - T_0)} \times 10^6 \quad (1)$$

where: f_T and f_{T_0} are the $\text{TE}_{01\delta}$ resonant frequencies at temperature T and T_0 , respectively.

3. Results and discussions

3.1. MoO_3 prepared via solid state reaction method

Relative ρ , ϵ_r and Q_f of MoO_3 ceramics prepared via solid state

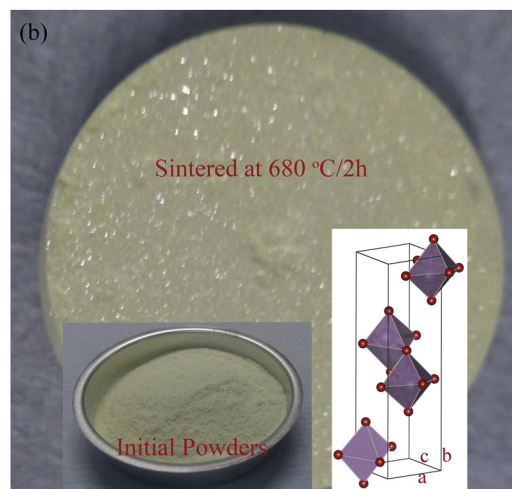
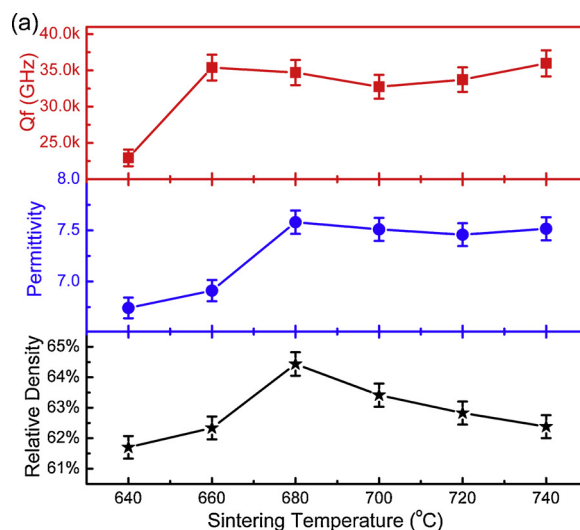


Fig. 1. a) Relative ρ , ϵ_r and Q_f value of MoO_3 ceramics prepared via conventional sintering as a function of sintering temperature ($640 \sim 740^\circ\text{C}$). b) Optical images of starting powders and MoO_3 ceramic sintered at $680^\circ\text{C} / 2\text{h}$ with its crystal structure inset.

reaction method as a function of sintering temperature ($640 \sim 740^\circ\text{C}$) are shown in Fig. 1a. ϵ_r increased from 6.75 to 7.58 as sintering temperature increased from 640°C to 680°C and then decreased a little bit with further increase in sintering temperature. Q_f reached a maximum value of 35,000 GHz at 660°C and remained almost constant for higher sintering temperatures. TCF was ~ -39 ppm/ $^\circ\text{C}$ and therefore the overall MW properties were similar to those reported [13]. Although the properties are attractive for the development of MW ceramics, MoO_3 pellets could not be well densified even at temperatures close to its melting point, only with a maximum relative $\rho \sim 64.5\%$ at 680°C . An optical image of an MoO_3 pellet sintered at 680°C and the schematic of crystal structure are shown in Fig. 1b. The pellet has a green-yellow color, similar to the starting powders. Conversely, some grains are observed which are $> 100\ \mu\text{m}$ in diameter which indicates that grain growth is possible but not uniform throughout the ceramic, resulting in poor mechanical strength and low fracture toughness. All the results suggest MoO_3 can not be well sintered using a conventional solid-state method even though high Q_f is observed. Moreover, its true ϵ_r is likely to be far higher than the measured value (~ 7.58).

3.2. MoO_3 prepared via cold sintering with water only

XRD patterns of the MoO_3 powders, the natural and fractured

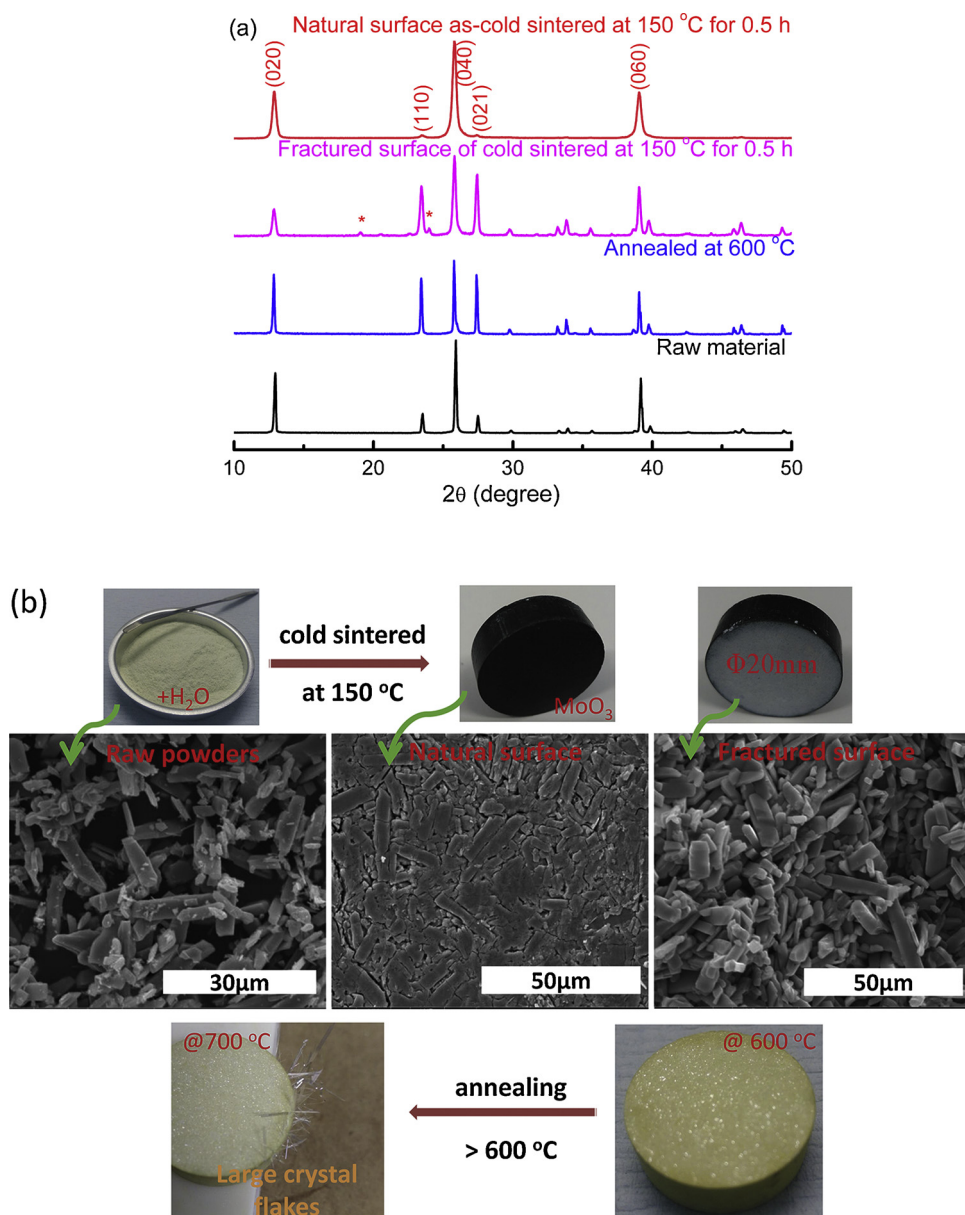


Fig. 2. a) XRD patterns of the raw MoO_3 powders, natural and fractured surfaces of cold sintered MoO_3 ceramic at $150\text{ }^\circ\text{C}$ for 0.5 h, and annealed sample $620\text{ }^\circ\text{C}$. b) Optical and SEM images of the starting powders and cold sintered MoO_3 ceramics.

surfaces of cold sintered MoO_3 ceramics (sintered 0.5 h at $150\text{ }^\circ\text{C}$) and a sample annealed at $620\text{ }^\circ\text{C}$ are shown in Fig. 2a. Scanning electron and optical images of starting powders and cold sintered MoO_3 ceramics are shown in Fig. 2b. The cold sintered MoO_3 ceramic is black in color on its surface but its interior is deep green. XRD results showed that besides MoO_3 , weak peaks of secondary phases were observed on the fracture surface, which indicates that some MoO_3 has reacted with H_2O forming secondary phases that did not decompose after 24 h drying at $150\text{ }^\circ\text{C}$. However, due to their low volume fraction they can not be identified. For the natural surface of the cold sintered MoO_3 ceramic, only XRD peaks of MoO_3 phase were observed but with evidence of some preferred orientation. The black surface color is attributed to reduction in the presence of heat, pressure and water. The starting powders adopt an acicular morphology (5 to $10\text{ }\mu\text{m}$) which is commensurate with an anisotropic crystal structure. The fracture surfaces of cold sintered MoO_3 ceramics show little grain growth compared with the starting powder. The black surface in contrast exhibits bar shaped grains in the a - c plane which are presumably responsible for the increase in intensity of the (020) and (040) peaks with respect to the

polycrystalline standard. After annealing above $300\text{ }^\circ\text{C}$, both the natural (outer) and fractured (interior) surfaces of cold sintered MoO_3 ceramic returned to the green-yellow color, the same with both that observed in the starting powder and for conventionally sintered MoO_3 ceramic. The relative ρ of MoO_3 ceramic cold sintered at $150\text{ }^\circ\text{C}$ was $\sim 76.8\%$ and increased to 77.4% and 78.7% at $600\text{ }^\circ\text{C}$ and $700\text{ }^\circ\text{C}$, respectively, with an improvement over conventionally sintered MoO_3 as shown in Fig. 3a. When cold sintered ceramics were annealed above $600\text{ }^\circ\text{C}$, large crystal flakes (whiskers) grew from the edge (Fig. 2b), this phenomenon was not observed in conventionally sintered MoO_3 ceramics. Whisker formation is often related to liquid or vapor phase transport and their formation could be driven by the evolution on annealing of H_2O from trapped OH^- groups. [24–26] ϵ_r and Q_f of the cold sintered MoO_3 ($150\text{ }^\circ\text{C}$) were ~ 8.31 and $\sim 900\text{ GHz}$ but increased to 9.02 and $19,700\text{ GHz}$, respectively, after annealing at $700\text{ }^\circ\text{C}$ as shown in Fig. 3b. TCF value of the cold sintered MoO_3 ceramic is about $-55 \pm 15\text{ ppm}/^\circ\text{C}$.

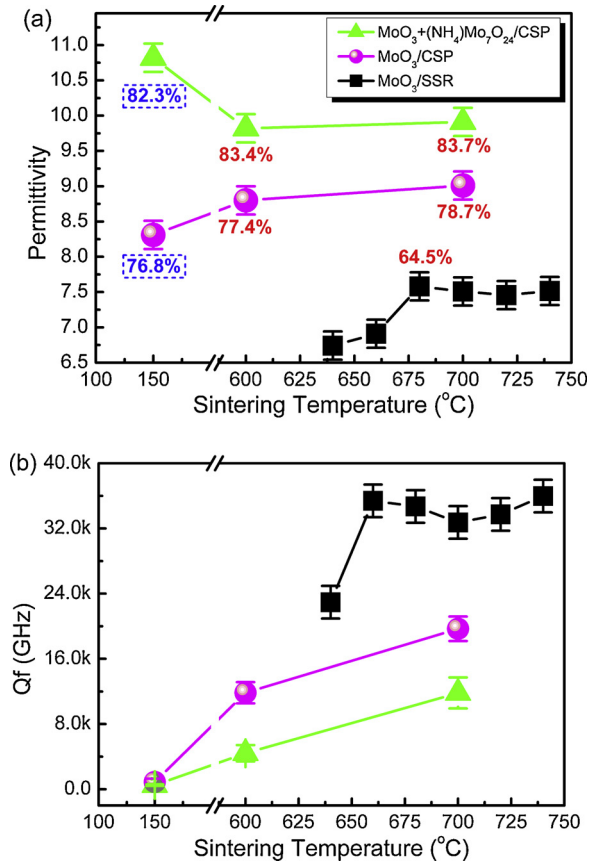
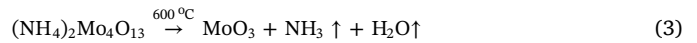
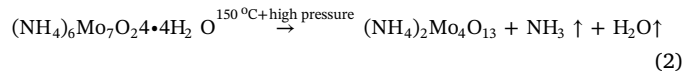


Fig. 3. a) Relative ρ_r , ϵ_r and b) Q_f of the MoO_3 prepared via conventional and cold sintering methods as a function of sintering temperature.

3.3. MoO_3 prepared by cold sintering with $(\text{NH}_4)_6\text{Mo}_7\text{O}_{24}\cdot 4\text{H}_2\text{O}$

Although cold sintering with H_2O improved relative ρ , the optimum value (78.7%), as shown in Fig. 3a, was below the required density for commercially useful MW ceramics ($> 95\%$). $(\text{NH}_4)_6\text{Mo}_7\text{O}_{24}\cdot 4\text{H}_2\text{O}$ is soluble in water and its re-crystallization may enhance densification during cold sintering. Hence, 10 wt. % $(\text{NH}_4)_6\text{Mo}_7\text{O}_{24}\cdot 4\text{H}_2\text{O}$ was mixed with MoO_3 powders before 4 wt. % H_2O was added. XRD patterns of the $(\text{NH}_4)_6\text{Mo}_7\text{O}_{24}\cdot 4\text{H}_2\text{O}$ powders, mixtures of MoO_3 ceramic with $(\text{NH}_4)_6\text{Mo}_7\text{O}_{24}\cdot 4\text{H}_2\text{O}$ cold sintered for 0.5 h at 150°C and a cold sintered sample annealed at 600°C are shown in Fig. 4. As reported in literatures, the $(\text{NH}_4)_6\text{Mo}_7\text{O}_{24}\cdot 4\text{H}_2\text{O}$ decomposes to $(\text{NH}_4)_4\text{Mo}_5\text{O}_{17}$ at $\sim 130^\circ\text{C}$ and the latter decomposes to $(\text{NH}_4)_2\text{Mo}_4\text{O}_{13}$ at about 245°C

[22,23]. In cold sintered MoO_3 (150°C) sample, $(\text{NH}_4)_2\text{Mo}_4\text{O}_{13}$ phases were revealed in addition to those of the matrix phase but after annealing at 600°C , only MoO_3 phases are observed, suggesting the following reaction sequence:



The relative ρ of cold sintered MoO_3 ceramic with $(\text{NH}_4)_6\text{Mo}_7\text{O}_{24}\cdot 4\text{H}_2\text{O}$ (150°C) addition was 82.3% but the presence of $(\text{NH}_4)_2\text{Mo}_4\text{O}_{13}$ secondary phase affects this value since it has a lower ρ (3.528 g/cm^3) [27] than that of MoO_3 (4.69 g/cm^3) as shown in Fig. 3a. ϵ_r of cold sintered MoO_3 with $(\text{NH}_4)_2\text{Mo}_4\text{O}_{13}$ as a secondary is ~ 10 , larger than that of pure MoO_3 . After annealing at 700°C , the relative ρ increased to its highest value (83.7%) but ϵ_r decreased to 9.91. Q_f value of cold sintered MoO_3 with $(\text{NH}_4)_6\text{Mo}_7\text{O}_{24}\cdot 4\text{H}_2\text{O}$ addition was only 500 GHz, but increased to 11,800 GHz after annealing at 700°C . TCF value of the annealed MoO_3 ceramics is about $-48 \pm 10 \text{ ppm}/^\circ\text{C}$, which is similar to the conventionally sintered MoO_3 ceramics.

3.4. Calculation of ϵ_r of MoO_3 using Shannon's additive rule

Based on the above results, we conclude that higher relative ρ results in higher ϵ_r but estimation of the true ϵ_r of MoO_3 ceramic with high porosity is inaccurate. From Shannon's additive rule, [28] polarizability at microwave region can be treated as the sum of both ionic and electronic components and the molecular polarizability (α) of complex substances maybe estimated by summing α of the constituent:

$$\alpha_{\text{MoO}_3} = \alpha_{\text{Mo}^{6+}} + 3\alpha_{\text{O}^{2-}} = 9.31 \text{ \AA}^3, \quad (4)$$

where the ionic polarizabilities of Mo^{6+} and O^{2-} are 3.28 \AA^3 and 2.01 \AA^3 , respectively [28,29], Considering the Clausius–Mosotti relation [30],

$$\epsilon_{\text{cal}} = \frac{3V + 8\pi\alpha}{3V - 4\pi\alpha} \approx 10.96 \quad (5)$$

where V is the cell volume ($202.95/4 = 50.74 \text{ \AA}^3$). The calculated permittivity is 10.96, larger than the measured maximum value ~ 9.91 . Shannon's additive rule usually gives good estimation for low permittivity materials and it is worth believing that the real permittivity of MoO_3 is around 11, which is 45% and 67% larger than the traditional one here and reported value, [13] respectively.

4. Conclusions

MoO_3 can not be well densified by conventional sintering with a

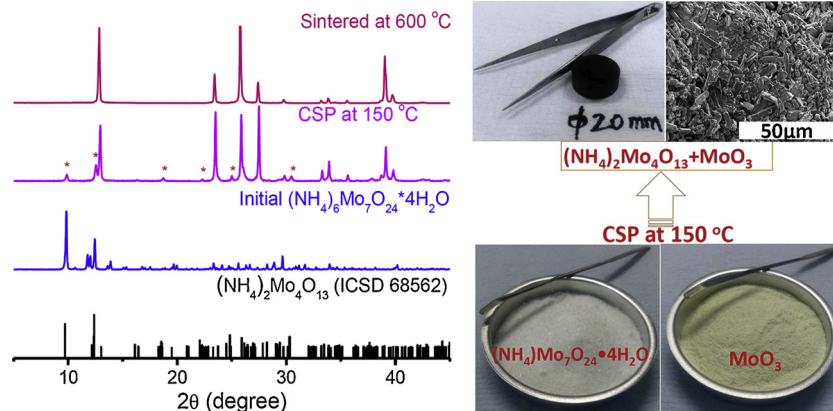


Fig. 4. XRD patterns of the starting $(\text{NH}_4)_6\text{Mo}_7\text{O}_{24}\cdot 4\text{H}_2\text{O}$ powder, cold sintered MoO_3 ceramic with $(\text{NH}_4)_6\text{Mo}_7\text{O}_{24}\cdot 4\text{H}_2\text{O}$ (150°C for 0.5 h) and a sample annealed at 600°C , and optical and SEM images of the starting powders and cold sintered MoO_3 ceramics.

relative $\rho \sim 64.5\%$ obtained at 680°C giving a $\epsilon_r \sim 7.58$, a $Qf \sim 35,000$ GHz and a $TCF \sim -39$ ppm/ $^\circ\text{C}$. Water-assisted cold sintering method increased the relative density of MoO_3 ceramic to $\sim 78\%$, which was further improved to $\sim 83\%$ by the addition of $(\text{NH}_4)\text{Mo}_7\text{O}_{24}\cdot 4\text{H}_2\text{O}$. However, higher temperature annealing was still required to eradicate secondary phases and / or and increase Qf . Calculated ϵ_r of MoO_3 using Shannon's additive rule is ~ 10.96 , which is 10% larger than that of the optimum cold sintered samples. Although relative ρ of MoO_3 did not achieve $> 95\%$, the methodology of introducing a cold sintering step for materials that are difficult to be sintered is adequately demonstrated.

Acknowledgements

This work was supported by Sustainability and Substitution of Functional Materials and Devices EPSRC (EP/L017563/1), the National Key Research and Development Program of China (2017YFB0406301), the National Natural Science Foundation of China (U1632146), the Key Basic Research Program of Shaanxi Province (2017GY-129), the Fundamental Research Funds for the Central University.

References

- [1] M.T. Sebastian, H. Jantunen, Low loss dielectric materials for LTCC applications: a review, *Int. Mater. Rev.* 53 (2008) 57–90.
- [2] H. Zhou, X. Liu, X. Chen, L. Fang, Y. Wang, $\text{ZnLi}_{2/3}\text{Ti}_{4/3}\text{O}_4$: a new low loss spinel microwave dielectric ceramic, *J. Eur. Ceram. Soc.* 32 (2012) 261–265.
- [3] Y.D. Zhang, D. Zhou, Pseudo phase diagram and microwave dielectric Properties of $\text{Li}_2\text{O-MgO-TiO}_2$ ternary system, *J. Am. Ceram. Soc.* 99 (2016) 3645–3650.
- [4] L.X. Pang, D. Zhou, Z.M. Qi, W.G. Liu, Z.X. Yue, I. Reaney, M.; Structure–property relationships of low sintering temperature scheelite-structured $(1-x)\text{BiVO}_4-x\text{LaNbO}_4$ microwave dielectric ceramics, *J. Mater. Chem. C* 5 (2017) 2695–2701.
- [5] L.X. Pang, D. Zhou, W.B. Li, Z.X. Yue, High quality microwave dielectric ceramic sintered at extreme-low temperature below 200 and co-firing with base metal, *J. Eur. Ceram. Soc.* 37 (2017) 3073–3077.
- [6] D. Zhou, L.X. Pang, D.W. Wang, C. Li, B.B. Jin, I.M. Reaney, High permittivity and low loss microwave dielectrics suitable for 5G resonators and low temperature co-fired ceramic architecture, *J. Mater. Chem. C* 5 (2017) 10094–10098.
- [7] D. Zhou, D. Guo, W.B. Li, L.X. Pang, X. Yao, D.W. Wang, I.M. Reaney, Novel temperature stable high- ϵ_r microwave dielectrics in the $\text{Bi}_2\text{O}_3\text{-TiO}_2\text{-V}_2\text{O}_5$ system, *J. Mater. Chem. C* 4 (2017) 5357–5362.
- [8] M.T. Sebastian, H. Wang, H. Jantunen, Low temperature co-fired ceramics with ultra-low sintering temperature: a review, *Curr. Opin. Solid State Mater. Sci.* 20 (2016) 151–170.
- [9] D.K. Kwon, M.T. Lanagan, T.R. Shrout, Microwave dielectric properties and low-temperature co-firing of BaTe_4O_9 with aluminum metal electrode, *J. Am. Ceram. Soc.* 88 (2005) 3419–3422.
- [10] L.X. Pang, D. Zhou, Modification of NdNbO_4 microwave dielectric ceramic by Bi substitutions, *J. Am. Ceram. Soc.* 00 (2019) 1–5, <https://doi.org/10.1111/jace.16290>.
- [11] N. Joseph, J. Varghese, T. Siponkoski, M. Teirikangas, M.T. Sebastian, H. Jantunen, Glass-free CuMoO_4 ceramic with excellent dielectric and thermal properties for ultralow temperature co-fired ceramic applications, *ACS Sustain. Chem. Eng.* 4 (2016) 5632–5639.
- [12] D. Zhou, L.X. Pang, Z.M. Qi, B.B. Jin, X. Yao, Novel ultra-low temperature co-fired microwave dielectric ceramic at 400 degrees and its chemical compatibility with base metal, *Sci. Rep.* 4 (2014) 5980.
- [13] J. Varghese, T. Siponkoski, M. Nelo, M.T. Sebastian, H. Jantunen, Microwave dielectric properties of low-temperature sinterable $\alpha\text{-MoO}_3$, *J. Eur. Ceram. Soc.* 38 (2018) 1541–1547.
- [14] D. Zhou, C.A. Randall, H. Wang, L.X. Pang, X. Yao, Microwave dielectric ceramics in $\text{Li}_2\text{O-Bi}_2\text{O}_3\text{-MoO}_3$ system with ultra-low sintering temperatures, *J. Am. Ceram. Soc.* 93 (2010) 1096–1100.
- [15] H. Sitepu, B.H. O'Connor, D. Li, Comparative evaluation of the March and generalized spherical harmonic preferred orientation models using X-ray diffraction data for molybdate and calcite powders, *J. Appl. Cryst.* 38 (2005) 158–167.
- [16] T. Leisegang, A.A. Levin, J. Walter, D.C. Meyer, In situ X-ray analysis of MoO_3 reduction, *Cryst. Res. Technol.* 40 (2005) 95–105.
- [17] J. Guo, A.L. Baker, H. Guo, M. Lanagan, C.A. Randall, Cold sintering process: a new era for ceramic packaging and microwave device development, *J. Am. Ceram. Soc.* 100 (2016) 669–677.
- [18] J. Guo, H. Guo, A.L. Baker, M.T. Lanagan, E.R. Kupp, G.L. Messing, C.A. Randall, Cold sintering: a paradigm shift for processing and integration of ceramics, *Angew. Chem. Int. Edit.* 55 (2016) 11457–11461.
- [19] H. Kahari, M. Teirikangas, J. Juuti, H. Jantunen, Improvements and modifications to room-temperature fabrication method for dielectric Li_2MoO_4 ceramics, *J. Am. Ceram. Soc.* 98 (2015) 687–689.
- [20] H. Kahari, M. Teirikangas, J. Juuti, H. Jantunen, Dielectric properties of Lithium molybdate ceramic fabricated at room temperature, *J. Am. Ceram. Soc.* 97 (2014) 3378–3379.
- [21] H. Kahari, M. Teirikangas, J. Juuti, H. Jantunen, Room-temperature fabrication of microwave dielectric $\text{Li}_2\text{MoO}_4\text{-TiO}_2$ composite ceramics, *Ceram. Int.* 42 (2016) 11442–11446.
- [22] T. Parsons, V. Maita, C. Lalli, *A Manual of Chemical and Biological Methods for Seawater Analysis*, Pergamon, Oxford, 1984.
- [23] H.T. Evans, B.M. Gatehouse, P. Leverett, Crystal Structure of the Heptamolybdate (VI) (paramolybdate) ion, $(\text{Mo}_7\text{O}_{24})^{6-}$, in the ammonium and potassium tetrahydrate salts, *Cheminform* (1975) 505–514.
- [24] D.Y. Geng, Z.D. Zhang, M. Zhang, D. Li, X.P. Song, K.Y. Hu, Structure and surface characterization of $\alpha\text{-MoO}_3$ whiskers synthesized by an oxidation process, *Scripta Mater.* 50 (2004) 983–986.
- [25] S. Phadungdhitidhada, P. Mangkorntong, S. Choopun, N. Mangkorntong, D. Wongratanaphisan, Synthesis of MoO_3 nanobelts by medium energy nitrogen ion implantation, *Mater. Lett.* 65 (2011) 568–571.
- [26] S. Phadungdhitidhada, P. Mangkorntong, S. Choopun, N. Mangkorntong, Raman scattering and electrical conductivity of nitrogen implanted MoO_3 whiskers, *Ceram. Int.* 34 (2008) 1121–1125.
- [27] R. Benchrif, M. le Blanc, R. de Pape, Synthesis and crystal structure of two polymorphs of $(\text{NH}_4)_2\text{Mo}_4\text{O}_{13}$, orthorhombic (o) and triclinic (t), *Eur. J. Solid State Inor. Chem.* 26 (1989) 593–601.
- [28] R.D. Shannon, Dielectric polarizabilities of ions in oxides and fluorides, *J. Appl. Phys.* 73 (1993) 348–366.
- [29] G.K. Choi, J.R. Kim, S.H. Yoon, K.S. Hong, Microwave dielectric properties of scheelite (A = Ca, Sr, Ba) and wolframite (A = Mg, Zn, Mn) AMoO_4 compounds, *J. Eur. Ceram. Soc.* 27 (2007) 3063–3067.
- [30] P.V. Ryssselberghe, Remarks concerning the Clausius–Mossotti law, *J. Phys. Chem.* 36 (1932) 1152–1155.